

EVALUATION OF MECHANICAL AND FRACTURE CHARACTERISTICS USING INSTRUMENTED INDENTATION TECHNIQUE

Jung-Suk Lee^{1,a}, Kwang-Ho Kim^{2,b}, Jea-Hwan Han^{1,c} and Dongil Kwon^{1,d}

¹School of Materials Science and Engineering, Seoul National University,
Seoul 151-744, Korea

²Research Institute of Advanced Materials, Frontics, Inc., Seoul 151-744, Korea

^ajslee119@plaza.snu.ac.kr, ^bkhkim@frontics.com, ^cione1@snu.ac.kr, ^ddongilk@snu.ac.kr

Keywords: Indentation; Flow properties; Residual stress; Fracture toughness; Weldment

Abstract. The material characterization on the weak points of the structural systems is essential to evaluate safety accurately. However, general material characterization methods such as uniaxial tensile test and CTOD (crack tip opening displacement) test are destructive, therefore, it cannot be applied to the system in use. To overcome this problem, the material characterization using instrumented indentation technique was developed. However, current researches on instrumented indentation technique focus on the hardness measurement. The evaluation of flow property, residual stress and fracture toughness using instrumented indentation technique is not sufficiently performed. In this paper, we introduce the evaluation method of the flow property, the residual stress near the weldment and the fracture toughness developed from damage mechanics. The algorithm of flow property evaluation, the residual stress evaluation model and the fracture toughness model by using indentation were verified comparing with the experimental results.

Introduction

Failure assessment for components of engineering structures is important for both service life extension and to minimize the potential for premature catastrophic failure. A variety of criteria for failure assessment such as crack-growth-typed failure and material-degradation-typed failure criterion require mechanical properties (flow properties, residual stress and fracture toughness) of target material in order to be carried out the quantitative and accurate assessment. Since conventional methods for mechanical properties cannot be applied to in-service structures due to their destructive nature, instrumented indentation technique (IIT) was adopted to evaluate in-situ material properties of them. From extracting the representative stress and strain by resolving stress-strain field beneath indenter tip, flow properties can be characterized [1], and residual stress can be evaluated by analyzing shift in indentation load-depth curve due to residual stress evolution [2]. In case of evaluation of fracture toughness, we suggest a new instrumented indentation model for estimating fracture toughness of ductile materials. This model is based on two key concepts. First, the indentation energy to the characteristic fracture initiation point during indentation may be closely related to a material's resistance to fracture, i.e., fracture toughness. Second, the characteristic fracture initiation point can be determined by exploiting the basic concepts of continuum damage mechanics (CDM). To verify the applicability of the suggested model, indentation tests and conventional fracture toughness tests were performed on several ductile steels. The estimated fracture toughness values obtained from the indentation technique were compared well with those from conventional fracture toughness tests.

Indentation-Derived Mechanical Properties

Derivation of Tensile Properties Extracting Representative Stress and Strain

The contact mean pressure, P_m is expressed as:

$$P_m = \frac{L_{\max}}{\pi a^2} \quad (1)$$

where L_{\max} is indentation load and a is contact radius obtained from indentation curve analysis [1]. An equivalent strain, ε_R of indentation is defined from the material displacement beneath the indenter along the indentation axis direction. The equivalent strain is expressed in Eq. (2) at the position of the contact radius by multiplying a fitting constant α . The value of α is used as 0.1 for various steels [1].

$$\varepsilon_R = \frac{\alpha}{\sqrt{1-(a/R)^2}} \frac{a}{R} \quad (2)$$

In case of metals including structural steels, the elastic and elastic/plastic deformation stages occurred at very low indentation load. Therefore, we considered only the plastic deformation region in this study. The equivalent stress, σ_R can be evaluated using the relationship with contact mean pressure as shown in Eq. (3) [1].

$$\frac{P_m}{\sigma_R} = \psi \quad (3)$$

where ψ is a constraint factor for plastic deformation and the upper limit is about 3 for fully plastic deformation of steels. The exact value of work-hardening exponent, equivalent stress and strain is calculated by iteration process.

Both equivalent stress and strain values are determined from the analysis of each unloading curve. The stress and strain relation is fitted as the Hollomon equation expressing work-hardening behavior. The fitted curve was extrapolated to initial yield and ultimate tensile regions. Then, yield strength was evaluated by inputting yield strain to the Hollomon equation. The ultimate tensile strength was evaluated using the concept that uniform elongation is equal to work-hardening exponent.

Evaluation of Residual Stress Using the Stress-Insensitive Contact Hardness Model

The residual stress in a welded joint can be evaluated by dividing the residual-stress-induced normal load, L_{res} by the contact area, A_c , regardless of the stress state [2]:

$$\sigma_{res} = \frac{\alpha}{\psi} L_{res} / A_c \quad (4)$$

where α is a constant related to the stress directionality of biaxial residual stress, and ψ is plastic constraint factor of which value is approximately 3.0. The biaxial stress state, in which $\sigma_y = k\sigma_x$, can be divided into a mean stress term and plastic-deformation-sensitive shear deviatoric term [2]:

$$\begin{array}{c} \text{Biaxial stress} \\ \left(\begin{array}{ccc} \sigma_{res}^x & 0 & 0 \\ 0 & \sigma_{res}^y & 0 \\ 0 & 0 & 0 \end{array} \right) \end{array} = \begin{array}{c} \text{Mean stress} \\ \left(\begin{array}{ccc} \sigma_{res}^x & 0 & 0 \\ 0 & k\sigma_{res}^x & 0 \\ 0 & 0 & 0 \end{array} \right) \end{array} = \begin{array}{c} \text{Mean stress} \\ \left(\begin{array}{ccc} \frac{(1+k)}{3}\sigma_{res}^x & 0 & 0 \\ 0 & \frac{(1+k)}{3}\sigma_{res}^x & 0 \\ 0 & 0 & \frac{(1+k)}{3}\sigma_{res}^x \end{array} \right) \end{array} + \begin{array}{c} \text{Deviatoric stress} \\ \left(\begin{array}{ccc} \frac{(2-k)}{3}\sigma_{res}^x & 0 & 0 \\ 0 & \frac{(2k-1)}{3}\sigma_{res}^x & 0 \\ 0 & 0 & -\frac{(1+k)}{3}\sigma_{res}^x \end{array} \right) \end{array} \quad (5)$$

The stress component parallel to the indentation axis in the deviatoric stress term ($\sigma_{33} = -(1+k)\sigma_{res}^x/3$) directly affects the indenting plastic deformation. A residual stress-induced normal load L_{res} can be defined from the selected deviator stress component as:

$$L_{res} = \psi \frac{(1+k)}{3} \sigma_{res}^x A_c \quad (6)$$

Therefore, α in Eq. (4) can be taken as approximately 1.5 in the equi-biaxial stress state. In the instrumented indentation test, the contact area is determined by unloading curve analysis. By differentiation of the power-law-fitted unloading curve at maximum indentation depth, the contact depth and contact area A_c can be calculated from the contact depth based on the geometry of the Vickers indenter [3].

$$A_c = 24.5h_c^2 \quad (7)$$

Thus residual stress was calculated from the analyzed contact area in Eq. (6) and the measured load change, L_{res}

Determination of Fracture Toughness Using Critical Indentation Energy Model

For a crack of length $2a$ in a finite plate, the fracture toughness is given by [4]:

$$K_{JC} = \sigma_f \sqrt{\pi a} \quad (8)$$

where σ_f is the remote tensile stress at fracture. According to Griffith theory, σ_f is given by [4]:

$$\sigma_f = \sqrt{\frac{2Ew_f}{\pi a}} \quad (9)$$

where E is the elastic modulus and w_f is the energy per unit area required to create a crack surface. Combining Eq. (8) and Eq. (9) yields the relationship between w_f and K_{JC} as

$$K_{JC} = \sqrt{2Ew_f} \quad (10)$$

To estimate K_{JC} using the indentation technique, w_f must be determined using only indentation parameters. Triaxiality ahead of the indenter tip is in the range 2~3, and the degree of constraint in the deformed indentation region is similar to that ahead of the crack tip [5-6]. Hence the indentation energy per unit contact area to the characteristic point can be related to w_f if there exists a characteristic fracture initiation point during the indentation process. This energy, henceforth called the critical indentation energy, is calculated from the indentation load-depth curve:

$$2w_f = \lim_{h \rightarrow h^*} \int_0^h \frac{4P}{\pi d^2} dh \quad (11)$$

where P is the applied load, h is the indentation depth, d is the chordal diameter of the impression and h^* is the critical indentation depth corresponding to the characteristic fracture initiation point. $2w_f$ indicates the formation of two crack surfaces.

Since there are no distinguishing marks that can be used to identify fractures occurring during indentation, h^* in Eq. (11) cannot be measured by direct methods (optical microscope or SEM observation). Thus to determine h^* , continuum damage mechanics (CDM) and critical void volume fraction were applied to the indentation process [7].

Experimental Procedures

To verify the indentation algorithm for flow properties, the natural gas transmission pipe was made by welding API X65 steel plates. The diameter and thickness of the pipe were 30 inch and 17.5mm, respectively. Seam welded pipe was welded each other circumferentially. The chemical compositions of API X65 base metal are 0.08C-0.019P-1.45Mn-0.003S-0.31Si (wt%). The circumferential girth weld joint was made by Gas Tungsten Arc Welding (GTAW) and Shielded Metal Arc Welding (SMAW) process with V-groove configuration. A mechanical test sample was obtained from the circumferential weld joint with the size of 10mm×50mm×17.5mm. The sample was ground with emery paper and finally polished with 1 μ m diamond paste.

In order to verify the indentation residual stress model, saw-cutting, hole drilling and indentation tests were carried out in SS400 and API X65 weld joints.

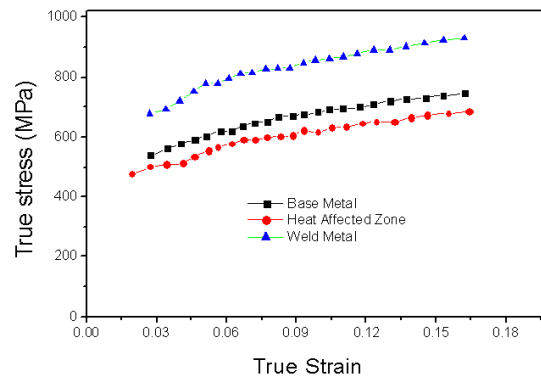
To verify the indentation fracture model, fracture toughness tests (CTOD tests) and indentation tests were performed for SUS303, SCM21, API X65 and X70, which have been widely used as structural steels

Results and Discussion

The boundary between heat-affected zone (HAZ) and base metal was identified 7mm from the fusion line using optical metallography and microhardness data for girth welded joint.



(a)



(b)

Fig. 1. Instrumented indentation test for API X60 pipeline under ground; (a) attached equipment to pipeline and (b) difference of flow properties with the change of microstructures.

Comparing the maximum indentation loads at the same indentation depth from the indentation load-depth curve, it was found the material resistance to deformation was high as the sequence of weld metal, base metal and HAZ. The true stress-strain behaviors were obtained from each indentation point. Generally, higher yield strengths were evaluated for weld metal and base metal than that of HAZ as expected from indentation load-depth curve. Especially, the yield strength of HAZ was lower than base metal as shown in Fig. 1. It is due to the softening phenomenon during welding process, generally observed in HAZ of thermo-mechanical control processed (TMCP) steel such as the steel used in this study [8-9]. And, HAZ can be identified as the weakest point for plastic deformation. The variation of yield strengths for outer, middle and inner lines are shown in Fig. 2 for the entire girth weld joint. The left part of the middle line has missing data due to the testing error by indenter slippage. The yield strengths of HAZ in the inner line were lower than those of HAZ in outer and middle lines. This phenomenon was explained by the annealing heat treatment of the constant heat input from outer welding paths.

Subsequently, to assess the reliability of the advanced indentation test, the true stress-strain properties of base metal from the instrumented indentation test was compared with the result from the uniaxial tensile test. The uniaxial tensile testing was done using the thin plate specimens obtained from 3 parts of thickness direction. The gauge length, width and thickness of the sample were 25 mm \times 6 mm \times 4 mm. The yield strengths of outer, middle and inner lines were 490, 440 and 495 MPa, respectively. And, the ultimate tensile strengths of outer, middle and inner lines were 628, 535 and 625 MPa, respectively. The flow properties from instrumented indentation testing are summarized below. The yield strengths of outer, middle and inner lines from instrumented indentation were 453, 451 and 467 MPa, respectively. The ultimate tensile strengths of outer, middle and inner lines were 718, 726 and 683 MPa, respectively. Based upon the comparison of the test results, it was determined that the instrumented indentation test can be successfully used for nondestructive evaluation of tensile properties.

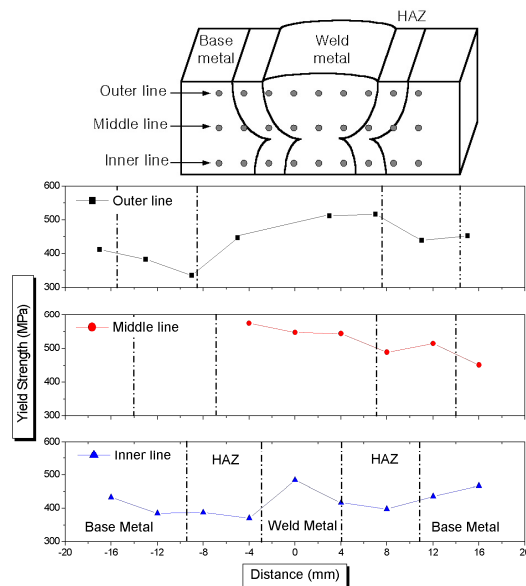


Fig. 2. Variation of the yield strengths for outer, middle and inner lines of the girth weld joint.

The welding residual stresses were obtained in the welded API X65 and SS400 pipelines using indentation, saw-cutting and hole-drilling methods. Here, the stress-free states were predicted from the flow stress ratio (which is independent of residual stress) of the weld metal or HAZ to base metal remote from weld-affected zone. In addition, the stress directionality factor k was pre-determined and non-equi-biaxial stress states could be considered. More detail on these procedures will be given in a later study. The results are shown in Fig. 3. The indentation results agree well with both kinds of reference test results. In particular, the most important tensile residual stresses in weld metal were almost identical in all tests. The results show that the instrumented indentation technique can be applied to nondestructive evaluation of residual welding stresses in industrial facility piping.

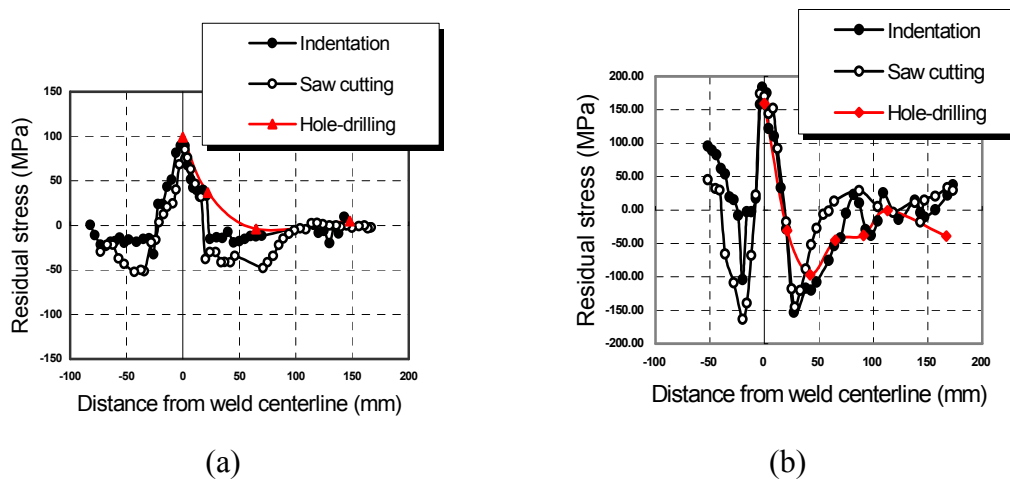


Fig. 3. Direct comparison of residual stresses measured by indentation technique with those obtained from saw-cutting and hole drilling tests; (a) SS400 and (b) API X65.

Table 1, listing h^* and K_{JC} values from the indentation technique and K_{JC} from the CTOD test, shows good agreement between K_{JC} from the indentation technique and from CTOD test. Here, h^* could be calculated by applying CDM and using the critical void volume fraction [7,10-11], and the following general equation was used to convert CTOD values to K_{JC} [12]:

$$K_{JC} = \sqrt{2\sigma_Y E \delta_{JC}} \quad (12)$$

The only a little discrepancy observed was for SCM21 and X70: the K_{JC} obtained using the indentation technique was slightly lower than that from the CTOD test, an error that might be reduced by obtaining a more accurate indentation load-depth curve (especially unloading part).

However, considering the standard deviation, the results in Table 1 are sufficiently accurate to show the validity of the critical indentation energy model.

Table 1. The values of fracture toughness from indentation and CTOD tests

Material	h^* (μm)	K_{JC} (Indentation) ($\text{MPam}^{0.5}$)	K_{JC} (CTOD) ($\text{MPam}^{0.5}$)
SUS303	122 ± 10.7	241 ± 22	251 ± 32
SCM21	121 ± 8.5	210 ± 15	261 ± 41
X65	195 ± 17.3	302 ± 23	300 ± 34
X70	190 ± 13.2	327 ± 17	380 ± 49

Summary

The instrumented indentation technique was used to evaluate the variation of the flow properties of an API X 65 girth welded joint, residual stress in SS400 and API X65 steel girth welded joints and the fracture toughness of the structural steels. The true stress-strain curves for the welded joint were evaluated based on the analysis of equivalent stress and strain considering the deformation behavior beneath the spherical indenter and indentation stress field. The degree of deformation resistance was compared for weld metal, HAZ and base metal with indentation load-depth curve and evaluated yield strength. Weld metal was identified as the highest value among the three regions. And, HAZ had the lowest value. Therefore, HAZ was the weakest point for plastic deformation. The yield strength and work-hardening exponent of API X65 base metal was nearly consistent with the results from the uniaxial tensile test.

Welding residual stresses were evaluated by the instrumented indentation technique based on the invariance of contact hardness regardless of residual stress, despite the shift in the indentation-loading curve with residual stress. The modeling of contact morphology and stress decomposition under a rigid indenter can explain the quantitative relation of residual stress and indentation load. To verify the indentation technique, welding residual stresses in SS400 and API X65 welded pipeline were evaluated and compared with reference saw-cutting and hole-drilling tests. Good agreement was found between the instrumented indentation and reference tests.

A new method for evaluating fracture toughness using indentation technique is presented. First, Griffith theory is used to develop a formula for evaluating fracture toughness from the critical indentation energy model. To verify the model, indentation and CTOD tests were performed for several structural steels. The test results show good agreement between K_{JC} from the indentation model and K_{JC} from CTOD test, boding well for practical use of the model in the future.

References

- [1] J.H. Ahn and D. Kwon: *J. Mater. Res.* Vol. 16 (2001), p. 3170
- [2] Y.H. Lee and D. Kwon: *Acta mater.* Vol. 52 (2004), p. 1555
- [3] W.C. Oliver and G.M. Pharr: *J. Mater. Res.* Vol. 7 (1992), p.1564
- [4] A.A. Griffith: *Phil. Trans. A* Vol. 221 (1920), p. 163
- [5] T.S. Byun, S.H. Kim, B.S. Lee, I.S. Kim and J.H. Hong: *J. Nucl. Mater.* Vol. 277 (2000), p. 263
- [6] H.A. Francis: *J. Engng. Mater. Tech.* Vol. 98 (1976), p. 272
- [7] J.S. Lee, J.I. Jang, B.W. Lee, Y. Choi, S.G. Lee and D. Kwon: *Acta Mater.* Vol. 54 (2005), p.1101
- [8] T. Mohandas, R.G. Madhusudan and K.B. Satish: *J. Mat. Proc. Tech.* Vol. 88 (1999), p. 284
- [9] R.G. Madhusudan and T. Mohandas: *J. Mat. Proc. Tech.* Vol. 57 (1996), p. 23
- [10] H. Andersson: *J. Mech. Phys. Solid* Vol. 25 (1977), p. 217
- [11] V. Tvergaard and A. Needleman: *Acta Metall.* Vol. 32 (1984), p. 157
- [12] ASTM Standard E1290, Standard Test Method for Plane-Strain Fracture Toughness of Metallic Materials (1993)